Published in final edited form as:
Plast Reconstr Surg. 2012 April ; 129(4): 838–847. doi:10.1097/PRS.0b013e3182450b47.

Regulation of Adipogenesis by Lymphatic fluid Stasis Part II: Expression of Adipose Differentiation Genes

Seth Aschen[1], **Jamie C. Zampell, MD**[1], **Sonia Elhadad, PhD**[1], **Evan Weitman, MD**[1], **Marina De Brot Andrade, MD**[2], and **Babak J. Mehrara, MD, FACS**[1]

[1]The Division of Plastic and Reconstructive Surgery, Memorial Sloan-Kettering Cancer Center, New York, NY 10065

[2]The Division of Breast Surgery, Department of Surgery, Memorial Sloan-Kettering Cancer Center, New York, NY 10065

Abstract

Background—Although fat deposition is a defining clinical characteristic of lymphedema, the cellular mechanisms that regulate this response remain unknown. The goal of this study was to determine how lymphatic fluid stasis regulates adipogenic gene activation and fat deposition.

Methods—Adult female mice underwent tail lymphatic ablation and sacrifice at 1, 3, or 6 weeks post-operatively (n=8/group). Samples were analyzed by immunohistochemistry and western blot. An alternative group of mice underwent axillary dissections or sham incisions and limb tissues were harvested 3 weeks post-operatively (n=8/group).

Results—Lymphatic fluid stasis resulted in significant subcutaneous fat deposition and fibrosis in lymphedematous tail regions ($p<0.001$). Western blot analysis demonstrated that proteins regulating adipose differentiation including CCAAT/enhancer binding protein-alpha (CEBP-α) and adiponectin were markedly upregulated in response to lymphatic fluid stasis in the tail and axillary models. Expression of these markers increased in edematous tissues according to the gradient of lymphatic stasis distal to the wound. Immunohistochemical analysis further demonstrated that adiponectin and peroxisome proliferator-activated receptor gamma (PPAR-γ), another critical adipogenic transcription factor, followed similar expression gradients. Finally, adiponectin and PPAR-γ expression localized to a variety of cell types in newly formed subcutaneous fat.

Conclusions—The mouse-tail model of lymphedema demonstrates pathological findings similar to clinical lymphedema including fat deposition and fibrosis. We show that lymphatic fluid stasis potently upregulates the expression of fat differentiation markers both spatially and temporally. These studies elucidate mechanisms regulating abnormal fat deposition in lymphedema pathogenesis and therefore provide a basis for developing targeted treatments.

Keywords

Lymph Stasis; inflammation; Lipogenesis; Peroxisome proliferator-activated receptor gamma (PPAR-γ); CCAAT/enhancer binding protein-alpha (CEBP-α); and adiponectin

Correspondence: Babak J. Mehrara, MD FACS, 1275 York Avenue, Suite MRI 1005, New York, NY 10021, 212-639-8639, 212-717-3677 (fax), mehrarab@mskcc.org.

Disclosures: None of the authors have any conflicts of interests or relevant disclosures to the findings presented in this study.

Introduction

Lymphedema is clinically characterized by progressive fat deposition and tissue fibrosis and may occur as a consequence of abnormalities in the lymphatic system or secondary to injury or disruption of lymphatic channels. Although recent studies have shown promising surgical treatments for lymphedema, treatment in most cases remains palliative, consisting of compression garments and manual lymphatic massage. Without these interventions, lymphedema often progresses with increasing fat deposition, deformity, and morbidity.

The cellular mechanisms that regulate fat deposition in lymphedema remain unknown. Thus, although it is clear that lymphatic injury is the initiating event, it remains unknown how changes in lymphatic fluid flow regulate adipose differentiation and proliferation. This gap in our knowledge is a significant barrier to the development of rational treatment and prevention options for lymphedema.

In part I of this study, we demonstrated that the mouse tail model of lymphatic fluid stasis results in histological changes that are similar to clinical lymphedema with significant subcutaneous fat deposition, fibrosis, and adipose tissue inflammation. The purpose of the current study was to determine how lymphatic fluid stasis regulates fat deposition. Specifically, we sought to determine how lymphatic fluid stasis regulates temporal and spatial expression patterns of genes critical for adipogenesis regulation. We show that lymphatic fluid stasis is associated with markedly increased expression of key adipogenic transcription factors including peroxisome proliferator-activated receptor gamma (PPAR-γ) and CCAAT/enhancer binding protein-alpha (CEBP-α), as well as the metabolically active protein adiponectin. Using mouse-tail and axillary dissection models, we show that spatial and temporal expression of these molecules depends on lymphatic fluid stasis and occurs in multiple cell types including stromal and inflammatory cells. Taken together, our results suggest that lymphatic fluid stasis is a key regulator of fat differentiation and that the mouse tail model is an excellent tool to study the molecular mechanisms of this response.

Methods

Mouse tail model

We used the mouse tail model to study the effect of lymphatic fluid stasis on expression of fat differentiation genes.(1–4) In this model, a dissecting microscope (StereoZoom SZ-4; Leica, Wetzlar, Germany) is used to excise a 2mm full-thickness circumferential segment of skin containing superficial capillary lymphatics 20mm distal to the base of the tail of 10–12 week old female C57BL/6 mice (Jackson Laboratory, Bar Harbor, Me). Deep collecting lymphatics adjacent to lateral tail veins are then individually identified and disrupted. Wounds were covered with Tegaderm dressings (3M, St. Paul, MN) for 5 days. Animals were sacrificed after 1, 3, or 6 weeks (n=8/group) for analysis. This model results in lymphatic fluid stasis persisting at least 6 weeks and demonstrates histological changes closely resembling clinical lymphedema including inflammation and fibrosis.(1–4)

Axillary lymph node dissection model

To confirm our findings in the tail model, we used our previously described mouse axillary lymph node dissection model.(4) We have shown that axillary lymph node dissection in mice results in modest, though significant, increases in upper and lower arm edema for as long as 3 weeks post-operatively.(4) Briefly, 10–12 week old adult female C57BL/6 mice (n=8/group) underwent axillary lymphadenectomy or sham operations (axillary incision without lymph node removal). Lymph nodes were identified by Evan's blue dye uptake (10 μl injection of 0.1% Evan's blue in palmar skin, Sigma, St. Louis, MO). Incisions were closed with absorbable suture and animals recovered. Skin and subcutaneous tissues were

harvested from upper and lower portions of the arm 3 weeks post-operatively, and total cellular protein was harvested as outlined below. Animal experiments were approved by the Institutional Animal Care and Use Committee and Resource Animal Research Center at Memorial Sloan-Kettering Cancer Center.

Western blot analysis

Protein was extracted from skin and subcutaneous tissues of the tail and upper extremity using our described methods.(4) To determine spatial changes in the expression of fat differentiation markers in response to lymphatic fluid stasis, tissues were harvested from tail regions corresponding to those analyzed histologically (i.e. 20 mm proximal or 20 and 30 mm distal to the zone of lymphatic disruption) 6 weeks after surgery. Protein was similarly harvested from upper and lower arms (5 mm proximal or distal to the elbow, respectively) of animals that had undergone sham or axillary lymph node dissection. To evaluate temporal changes in adipogenic gene expression in response to lymphatic fluid stasis, we harvested tissues in distal tail regions (30 mm distal to the zone of lymphatic obstruction) 1, 3, and 6 weeks post-operatively.

For protein extraction, 5 mm full-thickness tissue sections were harvested (n=3–5 animals/group per time point), frozen in liquid nitrogen, and homogenized. Total cellular protein was extracted using Tissue Protein Extraction Reagent (T-PER, ThermoFisher Scientific, Rockford, IL) and quantified using the Bradford technique (Bio-Rad Protein Assay, Hercules, CA). Proteins (4–6 μg) were separated on 10% SDS-polyacrylamide gel by electrophoresis (1X Tris-glycine/0.1% SDS buffer) and transferred to polyvinylidene fluoride membrane (Bioexpress, Kaysville, UT). Membranes were blocked using 5% non-fat milk in 1X Tris-buffered Saline Tween20 (TBST) and incubated with primary antibodies against CEBP-α (Cell Signaling) or adiponectin (Abcam) followed by appropriate HRP-conjugated secondary antibody (Santa Cruz Biotechnology, Santa Cruz, CA). Staining was detected by ECL Plus Western Blotting Detection System (GE Healthcare, Little Chalfont, UK). Loading levels were equalized by β-actin (Abcam) staining. Experiments were repeated in triplicate and ImageJ software used to determine relative signal densities after normalization to actin as previously described (5).

Microlymphangiography

Microlymphangiography was performed to visualize gradients of lymphatic fluid stasis by injecting fluorescein isothiocyanate (FITC)-conjugated, lysine-fixable dextran (2,000 kDa, 2 mg/ml, Molecular Probes, Eugene, OR) intradermally into the distal portion of the tail (6). This molecule is too large to be taken up by the microvasculature and either remains in the interstitial fluid or transported in dermal lymphatics generating a “honey-comb” pattern in the skin. Images were acquired using a Leica MZ FLIII Stereofluorescence microscope (Leica Microsystems, Bannockburn, IL) and analyzed using Volocity software (PerkinElmaer, Waltham, MA).

Immunohistochemistry

Tail tissues were harvested 6 weeks after surgery and prepared for histological analysis using our described methods.(4) Briefly, we harvested 5 mm cross-sections located 20 and 30 mm distal to the zone of lymphatic obstruction (designated as $D^{+}20$ and $D^{+}30$, respectively) as well as 20 mm proximal to the wound site (designated as $P^{-}20$). This enabled direct comparison of tissue regions exposed to lymphatic fluid stasis (i.e. distal segments) to those exposed to normal lymphatic flow (i.e. proximal segments). Tissue sections were fixed in 4% paraformaldehyde, decalcified in Immunocal (Decal Chemical Corp, Tallman, NY), embedded in paraffin, and sectioned at 5 μm.

Immunohistochemical (IHC) staining was performed to localize cellular markers for adipose differentiation in tail tissues harvested 6 weeks after surgery using our published methods.(1) Briefly, slides were deparaffinized, rehydrated in graded alcohol, permeabilized in 0.3% Triton X-100 (Sigma, St. Louis, MO), boiled in 10mM citric acid for antigen retrieval, and quenched with 3.0% hydrogen peroxide to block endogenous peroxidase activity. Sections were blocked with 20% normal serum in 0.1M glycine/0.2% BSA/PBS at 37°C followed by incubation with rabbit polyclonal antibodies for PPAR-γ, collagen type I, or mouse monoclonal antibody for adiponectin (all from Abcam, Cambridge, MA). Control sections were incubated without primary antibody. Staining was detected using biotinylated secondary antibodies and avidin-peroxidase complex (Vectastain ABC kit, Vector Laboratories) followed by visualization with 3,3′ diaminobenzidine tetrahydrochloride (Dako, Carpinteria, CA). Slides were counterstained with Harris hematoxylin (Dako), dehydrated, and mounted. Tissue sections were visualized by bright-field microscopy (Axioscope 40, Carl Zeiss) and images captured using a Mirax slide scanner (Carl Zeiss).

To quantify staining for PPAR-γ or adiponectin, two blinded reviewers counted the number of positively stained cells in 6–7 hpf (40X) per section (n=4/group) in cross-sectional specimens. Additionally, a trained pathologist (MDB) evaluated the slides for identification of cell types that expressed PPAR-γ and adiponectin.

Statistical analysis

Statistical analysis of multiple groups was performed using one-way ANOVA with the Tukey-Kramer multiple comparison *post-hoc* test with $p<0.05$ considered significant. Results are reported as mean ± standard deviation unless otherwise noted.

Results

Gradients of lymphatic fluid stasis regulate expression of fat differentiation genes

To determine the molecular mechanisms that regulate fat differentiation in response to lymph stasis, we performed western blot analysis of fat differentiation genes from different regions of the tail 6 weeks after surgery (Figure 1A). CEPB-α is a critical transcription factor that is required for fat differentiation and commitment of cells to the adipocyte lineage.(7) CEPB-α was increased in regions of the tail exposed to lymphatic fluid stasis (i.e. distal to the zone of lymphatic disruption) as compared to proximal regions. Expression was increased to the greatest extent in the region of the tail located closest to the zone of lymphatic disruption (D^+20; 2.4-fold increase) and slightly decreased in more distal regions (D^+30; 2.1-fold increase). These changes corresponded with gradients of lymphatic fluid stasis in the distal tail as evidenced by microlymphangiography (Figure 1B).

A similar expression pattern was present for adiponectin, a metabolically active hormone peptide that is essential for adipocyte differentiation (Figure 1A). Adiponectin expression was greatest in tail regions located closest to the zone of lymphatic obstruction (D^+20; 2.2-fold increase) and also slightly decreased in more distal regions (D^+30; 1.7-fold increase). Taken together, these findings show that tissues exposed to lymphatic fluid stasis have upregulated expression of fat differentiation genes (i.e. proximal vs. distal comparison) and that gradients of lymphatic fluid stasis contribute to this response (i.e. D^+20 vs. D^+30) since the regions of distal tail closest to the wound are exposed to the highest degree of lymph stasis.

To confirm our findings in a more physiologically relevant model, we performed axillary dissection or sham incisions in mice and harvested protein from upper and lower portions of the arm. We have shown that this procedure results in modest increases in arm volume, although the degree of swelling is markedly less than achieved by the tail model, thereby

corresponding to less severe lymphatic fluid stasis.(4) Similar to our findings with the tail model, CEPB-α expression was increased in the upper extremity subjected to axillary lymph node dissection (ALND; 1.4 and 1.5-fold increase compared to sham; Figure 2A, B). Similarly, adiponectin expression was increased in the upper extremity subjected to ALND (1.6 and 1.2-fold increase in upper and lower regions of the arm, respectively). These changes are distinct from post-surgical changes resulting from the skin incision alone since control animals also had an axillary incision. Similar to our observations in the tail model, we noted that the expression of adiponectin, and to a lesser extent CEPB-α were increased in the upper region of the arm as compared to the more distal portions, thereby corresponding to the gradients of lymphatic stasis in the upper extremity after axillary lymph node dissection (i.e. highest degree of stasis in the region of the arm closest to the zone of lymphatic obstruction).

Expression of fat differentiation markers is increased temporally with sustained lymphatic fluid stasis

We next sought to determine if changes in expression of fat differentiation markers corresponded to the length of time tissues were exposed to lymphatic fluid stasis. Mice underwent tail lymphatic ablation and tissues located distal to the zone of lymphatic injury ($D^{+}20$) were harvested after 1, 3, and 6 weeks. We have shown in the mouse tail model that inflammatory changes resulting from lymphatic fluid stasis begin 2 weeks post-operatively and reach maximum levels by 6 weeks.(1, 3) Corresponding to this pattern of inflammation, we found that CEPB-α expression increased over time such that expression at 3 and 6 weeks were 6.4-fold and 8.4-fold higher, respectively, compared to 1 week specimens (Figure 3). Similarly, adiponectin expression was increased 2.7-fold and 6.3-fold at 3 and 6 week time points when compared to 1 week. These findings suggest that expression of fat differentiation genes is upregulated in response to prolonged exposure to lymphatic fluid stasis.

Gradients of lymphatic fluid stasis regulate the expression of fat differentiation genes in inflammatory and stromal cells

We performed immunohistochemistry to localize the expression of fat differentiation genes in response to lymphatic fluid stasis. We attempted to localize CEPB-α, however, multiple trials with different antibodies and antigen unmasking efforts were unsuccessful. Therefore, we focused attention on peroxisome proliferator-activated receptor gamma (PPAR-γ), a transcription factor that is activated by CEPB-α, required for commitment to fat differentiation, and necessary for maintenance of adipocyte phenotype.(7) This analysis, consistent with our western blot studies, demonstrated that PPAR-γ expression is regulated by gradients of lymphatic fluid stasis such that distal tail regions exposed to lymph stasis had significantly more PPAR-γ expression as compared with proximal, non-edematous regions (Figure 4A–D). This difference could be easily seen by histological examination and were highly statistically significant when quantified by cell counts (3-fold increase at $D^{+}20$; $p<0.001$; Figure 4A). PPAR-γ+ cells localized to the subcutaneous fat, perivascular regions, and regions surrounding the basal layer of hair follicles (Figure 5). Although the vast majority of PPAR-γ+ cells were mononuclear cells, PPAR-γ expression was noted in a wide variety of cell types including adipocytes, lymphocytes, pericytes, cells surrounding nerve sheaths, fibroblasts, and lymphatic endothelial cells (Figure 5A–D).

Localization of adiponectin demonstrated similar results. Clear gradients of expression of adiponectin could be observed when comparing regions proximal and distal to the zone of lymphatic obstruction (Figure 6). Although low-level expression of adiponectin was noted in proximal tail regions, we noted a nearly 3-fold increase in the number of adiponectin+ cells in distal regions (Figure 6A–C; $p<0.001$). Again, expression was localized to mononuclear

cells primarily in subcutaneous fat. Infiltrating inflammatory cells expressed adiponectin as well as a variety of other cell types including adipocytes, pericytes, cells of the nerve sheath, fibroblasts, and macrophages (Figure 7). Contrary to PPAR-γ, we did not note adiponectin expression in lymphatic or microvascular endothelial cells.

Discussion

In the current study, we show that gradients of lymphatic fluid stasis regulate the expression of CEPB-α and PPAR-γ and that the expression of these molecules correlates temporally and spatially with fat deposition in response to lymphatic fluid stasis. The expression of CEPB-α was markedly increased in regions of the tail or axilla distal to the zone of lymphatic obstruction. Similarly, in the tail model, PPAR-γ expression localized histologically to the hypertrophic subcutaneous fat. These findings are important and suggest that lymphatic fluid stasis can either directly or indirectly activate expression of CEPB-α and PPAR-γ thereby regulating lipid accumulation. This hypothesis is supported by previous studies demonstrating that CEPB-α and PPAR-γ are master regulators of adipogenesis that control adipocyte differentiation, proliferation, and lipid accumulation.(8) Although CEPB-α is required for activation of PPAR-γ, the latter is the dominant transcription factor in adipogenesis, as continuous expression of PPAR-γ is necessary for maintenance of adipocyte differentiation and lipid accumulation.(9, 10) In addition, activation of PPAR-γ by CEPB-α results in a positive feedback loop, thereby accelerating adipogenesis.(8) PPAR-γ is a critical regulator of many fat-selective genes and directly binds to and regulates their expression.(11) Exogenous expression of PPAR-γ can promote adipogenesis in fibroblasts and myoblastic cell lines.(12) Thus, it is possible that lymphatic fluid stasis activates expression of CEPB-α which in turn activates PPAR-γ initiating a positive feedback loop ultimately resulting in adipogenesis in the subcutaneous compartment. Further, based on our immunohistochemical localization of PPAR-γ we can speculate that induced expression of this transcription factor results in adipose differentiation of local tissues since we noted PPAR-γ expression in a variety of cell types.

In our histological analysis we noted that PPAR-γ expression by macrophages localized to the subcutaneous fat compartment. This finding is important, as PPAR-γ is a critical regulator of macrophage differentiation and plays an important role in insulin resistance and expression of pro-inflammatory cytokines in obese mice.(13, 14) Therefore, it is possible that expression of PPAR-γ by macrophages in response to lymphatic fluid stasis promotes the expression of inflammatory cytokines and contributes to the adipose tissue inflammation we have previously observed.

Lymphatic fluid stasis increased adiponectin expression both temporally and spatially. Adiponectin is a peptide hormone that is a late marker of activated adipocytes but is also expressed by other mesenchymal cells and inflammatory cells.(15) Adiponectin expression is highest in periods of lipid accumulation and decreases with adipose tissue hypertrophy and hypoxia.(16) This pattern is consistent with our finding that adiponectin expression increased temporally and correlated with fat accumulation in the mouse tail model. Increased adiponectin expression in our study is also likely a correlate of tissue inflammation, since adiponectin was expressed by inflammatory cell types including mononuclear cells and macrophages in regions distal to the zone of lymphatic obstruction. This hypothesis is supported by previous studies demonstrating that, in addition to regulating lipid storage in fat cells (16), adiponectin also contributes to cell signaling between adipose and immune cells, limiting chronic inflammatory reactions (15), and mediating macrophage activation by a variety of molecular pathways.(15) Thus, adiponectin expression in response to lymphatic fluid stasis may have complex effects initiating inflammatory responses in the early phases and mediating tolerance to additional pro-

inflammatory stimuli in the later phases of lymphatic obstruction. This hypothesis is supported by previous studies demonstrating that exposure of macrophages to adiponectin can result in macrophage activation (17) but that adiponectin stimulation can decrease monocytes adhesion to the endothelium (18, 19) and decrease macrophage activation in response to other stimuli. (20)

Our current study does not elucidate precisely how lymphatic fluid stasis regulates the expression of adipogenic differentiation genes. It is not clear, for example, whether this effect is a direct activation of PPAR-γ, CEPB-α, or adiponectin or if this response is related to secondary changes that occur in response to lymphatic fluid stasis. Our temporal analysis of CEPB-α and adiponectin suggest that this response is an indirect effect, since expression of these molecules increased with time after surgery. This is supported by our immunohistochemical studies localizing PPAR-γ and adiponectin to inflammatory cells as well as adipocytes, suggesting that inflammatory changes contribute to this process. Future studies will address this issue by determining the effect of immune modulation on fat deposition and adipocyte differentiation in response to lymphatic fluid stasis.

In conclusion, we have shown that lymphatic fluid stasis regulates the expression of adipocyte differentiation factors CEPB-α, PPAR-γ, and adiponectin both temporally and spatially. These responses occur even in response to minor alterations in lymphatic fluid transport capacity such as axillary lymph node dissection. Our results suggest that the mouse tail and axillary lymph node dissection models are useful means of analyzing the cellular and molecular responses that may be responsible for the pathological changes associated with lymphedema.

Acknowledgments

Grants

Sources of funding for this work are gratefully acknowledged and include an NIH T32 grant for JZ, Society of Memorial Sloan-Kettering Grant for salary support for SE and SA, Plastic Surgery Education Foundation Research Fellowship Grants for BJM, JCZ and TA, and the Sloan-Kettering Institute Department of Surgery.

References

1. Clavin NW, Avraham T, Fernandez J, et al. TGF-beta1 is a negative regulator of lymphatic regeneration during wound repair. Am J Physiol Heart Circ Physiol. 2008; 295:H2113–2127. [PubMed: 18849330]
2. Avraham T, Clavin NW, Daluvoy SV, et al. Fibrosis is a key inhibitor of lymphatic regeneration. Plast Reconstr Surg. 2009; 124:438–450. [PubMed: 19644258]
3. Avraham T, Daluvoy S, Zampell J, et al. Blockade of Transforming Growth Factor-{beta}1 Accelerates Lymphatic Regeneration during Wound Repair. Am J Pathol. 2010; 177:3202–3214. [PubMed: 21056998]
4. Zampell JC, Yan A, Avraham T, et al. Temporal and spatial patterns of endogenous danger signal expression after wound healing and in response to lymphedema. Am J Physiol Cell Physiol. 2011
5. Avraham T, Daluvoy S, Zampell J, et al. Blockade of transforming growth factor-beta1 accelerates lymphatic regeneration during wound repair. Am J Pathol. 177:3202–3214. [PubMed: 21056998]
6. Swartz MA, Berk DA, Jain RK. Transport in lymphatic capillaries. I. Macroscopic measurements using residence time distribution theory. Am J Physiol. 1996; 270:H324–329. [PubMed: 8769768]
7. Rosen ED, Hsu CH, Wang X, et al. C/EBPalpha induces adipogenesis through PPARgamma: a unified pathway. Genes & development. 2002; 16:22–26. [PubMed: 11782441]
8. Cook A, Cowan C. Adipose. 2008
9. Rosen ED. The molecular control of adipogenesis, with special reference to lymphatic pathology. Ann N Y Acad Sci. 2002; 979:143–158. discussion 188–196. [PubMed: 12543724]

10. Gesta S, Tseng YH, Kahn CR. Developmental origin of fat: tracking obesity to its source. Cell. 2007; 131:242–256. [PubMed: 17956727]
11. Tontonoz P, Hu E, Devine J, et al. PPAR gamma 2 regulates adipose expression of the phosphoenolpyruvate carboxykinase gene. Mol Cell Biol. 1995; 15:351–357. [PubMed: 7799943]
12. Hu E, Tontonoz P, Spiegelman BM. Transdifferentiation of myoblasts by the adipogenic transcription factors PPAR gamma and C/EBP alpha. Proc Natl Acad Sci U S A. 1995; 92:9856–9860. [PubMed: 7568232]
13. Heilbronn LK, Campbell LV. Adipose tissue macrophages, low grade inflammation and insulin resistance in human obesity. Curr Pharm Des. 2008; 14:1225–1230. [PubMed: 18473870]
14. Hevener AL, Olefsky JM, Reichart D, et al. Macrophage PPAR gamma is required for normal skeletal muscle and hepatic insulin sensitivity and full antidiabetic effects of thiazolidinediones. J Clin Invest. 2007; 117:1658–1669. [PubMed: 17525798]
15. Rocha VZ, Folco EJ. Inflammatory concepts of obesity. Int J Inflam. 2011; 2011:529061. [PubMed: 21837268]
16. Harford KA, Reynolds CM, McGillicuddy FC, et al. Fats, inflammation and insulin resistance: insights to the role of macrophage and T-cell accumulation in adipose tissue. Proc Nutr Soc. 2011:1–10.
17. Folco EJ, Rocha VZ, Lopez-Ilasaca M, et al. Adiponectin inhibits pro-inflammatory signaling in human macrophages independent of interleukin-10. J Biol Chem. 2009; 284:25569–25575. [PubMed: 19617629]
18. Ouchi N, Kihara S, Arita Y, et al. Novel modulator for endothelial adhesion molecules: adipocyte-derived plasma protein adiponectin. Circulation. 1999; 100:2473–2476. [PubMed: 10604883]
19. Ouedraogo R, Gong Y, Berzins B, et al. Adiponectin deficiency increases leukocyte-endothelium interactions via upregulation of endothelial cell adhesion molecules in vivo. J Clin Invest. 2007; 117:1718–1726. [PubMed: 17549259]
20. Okamoto Y, Folco EJ, Minami M, et al. Adiponectin inhibits the production of CXC receptor 3 chemokine ligands in macrophages and reduces T-lymphocyte recruitment in atherogenesis. Circ Res. 2008; 102:218–225. [PubMed: 17991878]

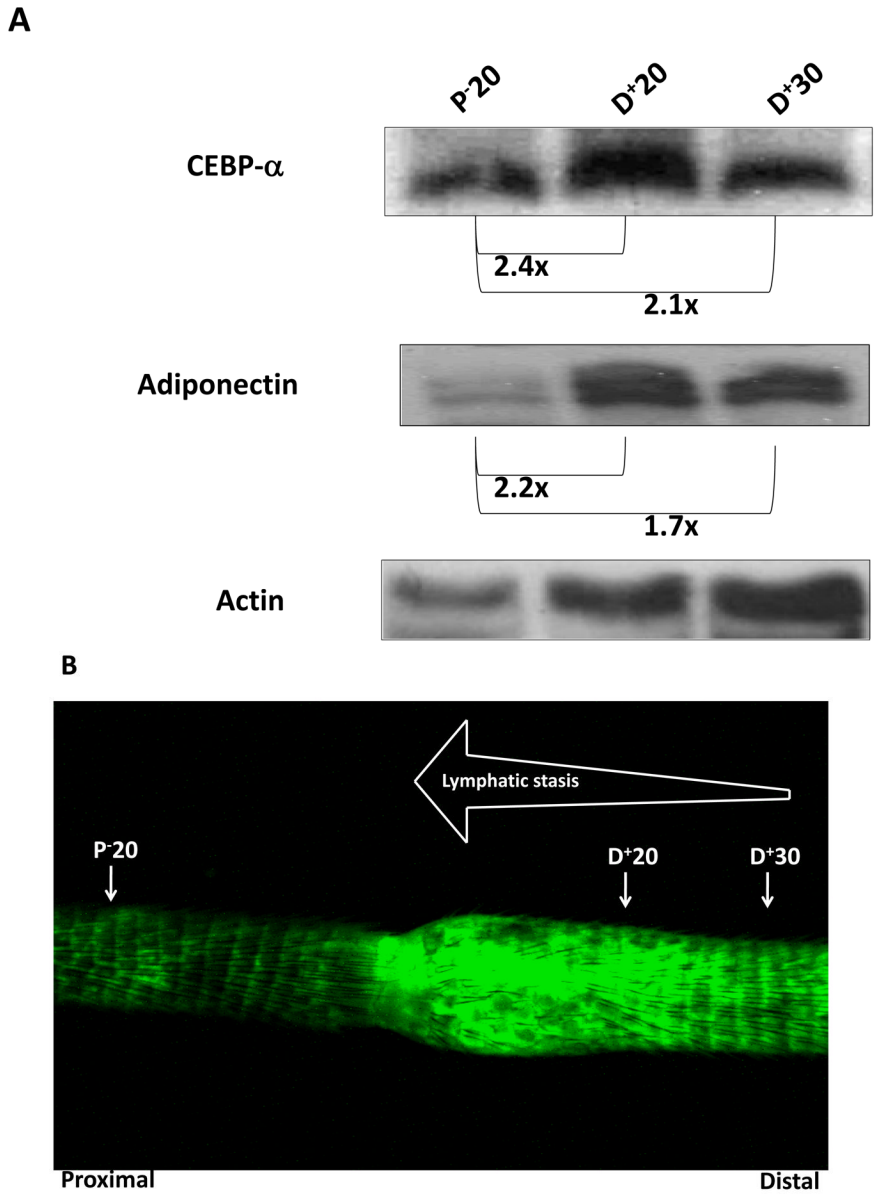

FIGURE 1. Gradients of lymphatic fluid stasis regulate expression of fat differentiation genes in the mouse tail model

A. Representative western blot (of triplicate studies) for CEPB-α, adiponectin, and actin in tissues harvested proximal ($P^{-}20$) or distal ($D^{+}20$ or $D^{+}30$) to the zone of lymphatic obstruction. Tissues were harvested 6 weeks following tail surgery. Fold changes relative to proximal region and corrected for actin using ImageJ software are shown for each western blot.

B. Representative microlymphangiography of the mouse tail 6-weeks after tail lymphatic excision demonstrating gradients of lymphatic fluid stasis in the distal regions of the tail (increasing fluorescent color). Also marked are the regions harvested for western blot analysis in A.

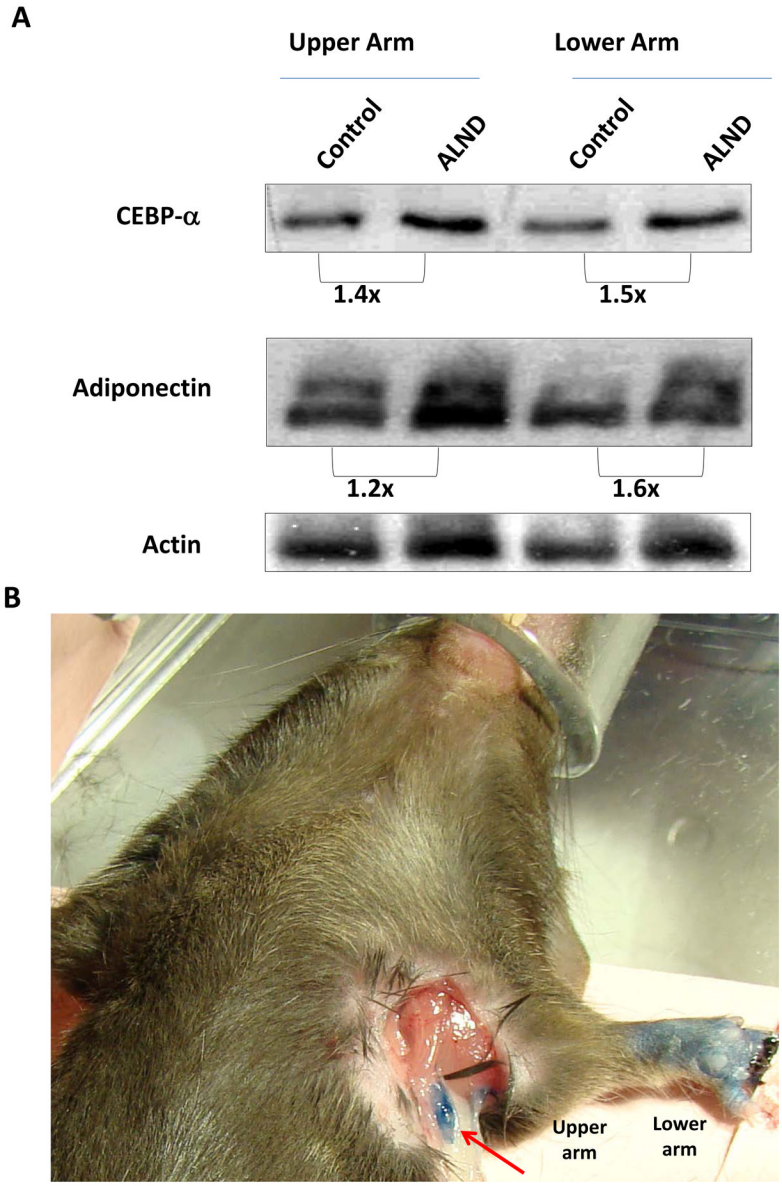

FIGURE 2. Gradients of lymphatic fluid stasis regulate expression of fat differentiation genes after axillary lymph node dissection

A. Representative western blot (of triplicate studies) for CEPB-α, adiponectin, and actin in tissues harvested from the upper or lower regions of the upper extremity in mice who had undergone control (incision only) or axillary lymphadenectomy (ALND). Fold changes relative to control and corrected for actin using ImageJ software are shown for each western blot.

B. Gross photograph of the mouse axillary dissection model demonstrating regions of the arm harvested for protein analysis. Also note blue lymph node (red arrow) in axilla.

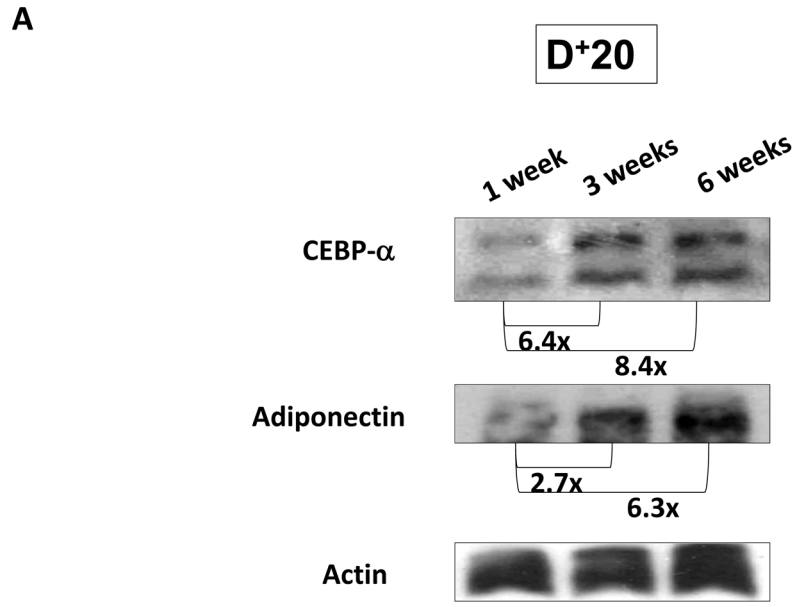

FIGURE 3. Expression of fat differentiation markers is increased temporally with sustained lymphatic fluid stasis

Representative western blot (of triplicate studies) for CEPB-α, adiponectin, IL-6, and actin in tissues harvested distal ($D^{+}20$) to the zone of lymphatic obstruction (gross photograph is shown for orientation to location of tissue harvest) 1, 3, or 6 weeks after surgery. Fold changes relative to 1 week time point and corrected for actin using ImageJ software are shown for each western blot.

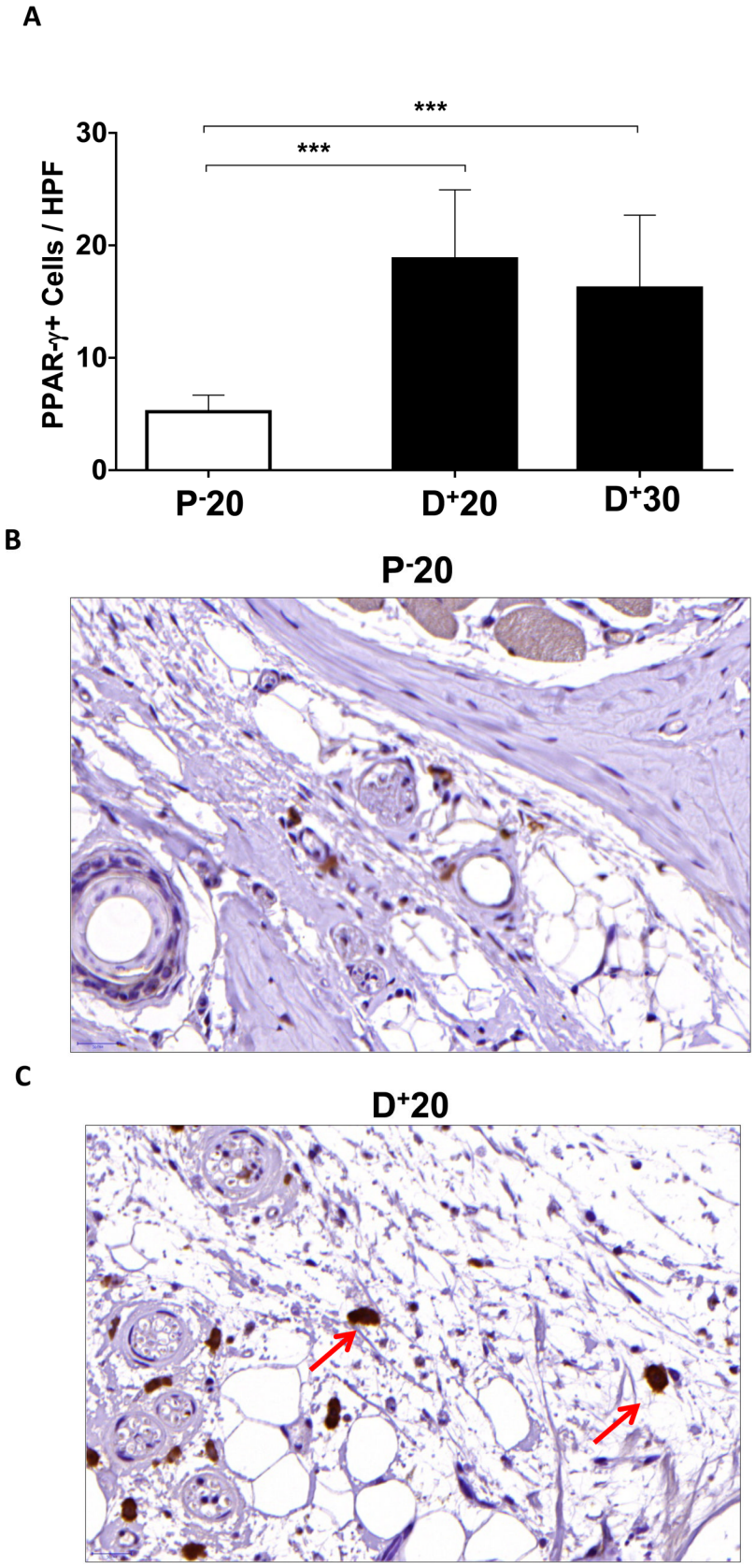

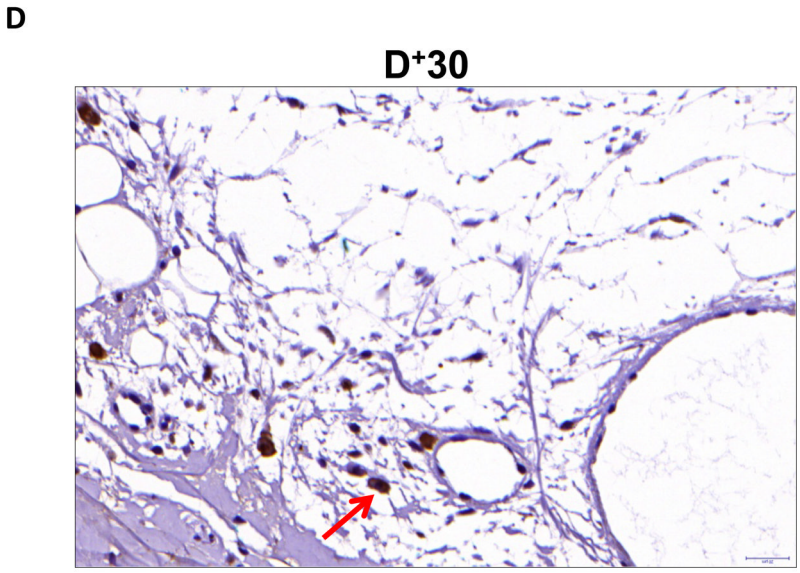

FIGURE 4. Gradients of lymphatic fluid stasis regulate the expression of PPAR-γ

A. PPAR-γ^+ cells/high powered field (HPF) cell counts in the various regions of the tail relative to the zone of lymphatic obstruction. Note significant increase in the number of PPAR-γ^+ cells/HPF in distal sections (***$p<0.001$).

B, C, D. Representative high (40x) images of cross-sectional regions of the mouse tail relative to the zone of lymphatic obstruction stained for PPAR-γ. Note increased number of positively stained cells in the distal regions. Also note staining of mononuclear cells in subcutaneous fat in distal regions (red arrows).

A

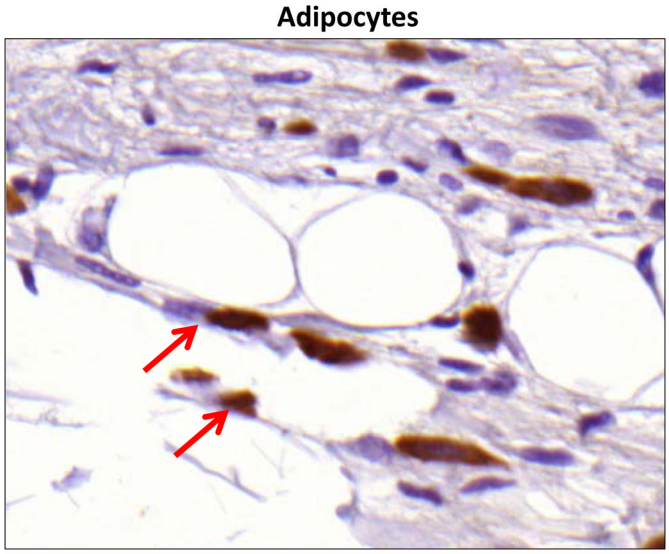

B

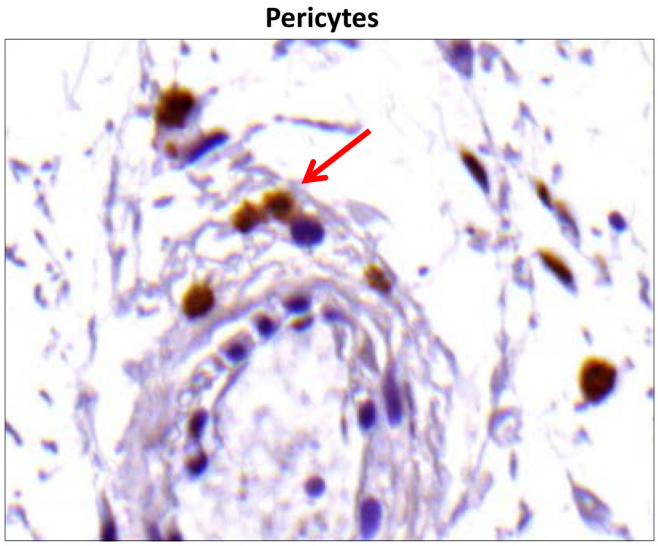

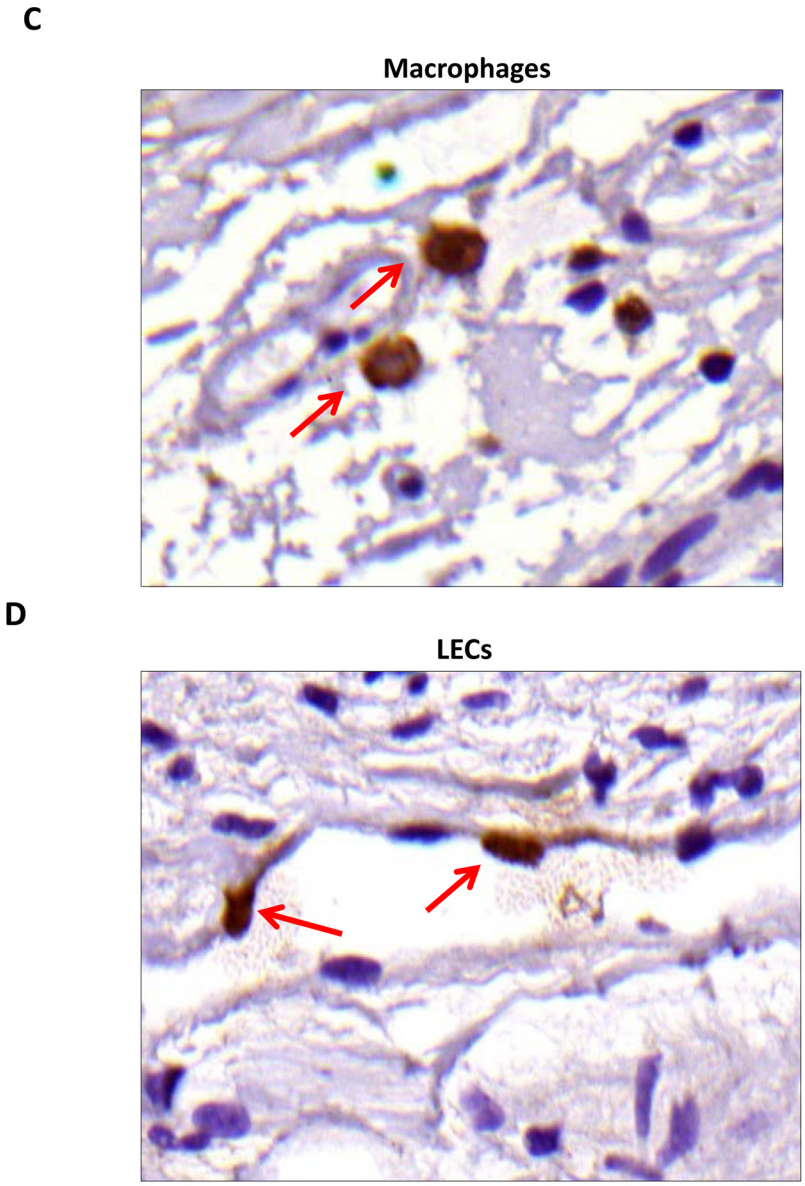

FIGURE 5. PPAR-γ is expressed by a variety of cell types in response to lymphatic fluid stasis

A–D. PPAR-γ staining (red arrows) of adipocytes (A), pericytes (B), macrophages (C), and lymphatic endothelial cells (LECS; D) shown in representative high power (80X) images of the distal region (D+20) of the tail.

A

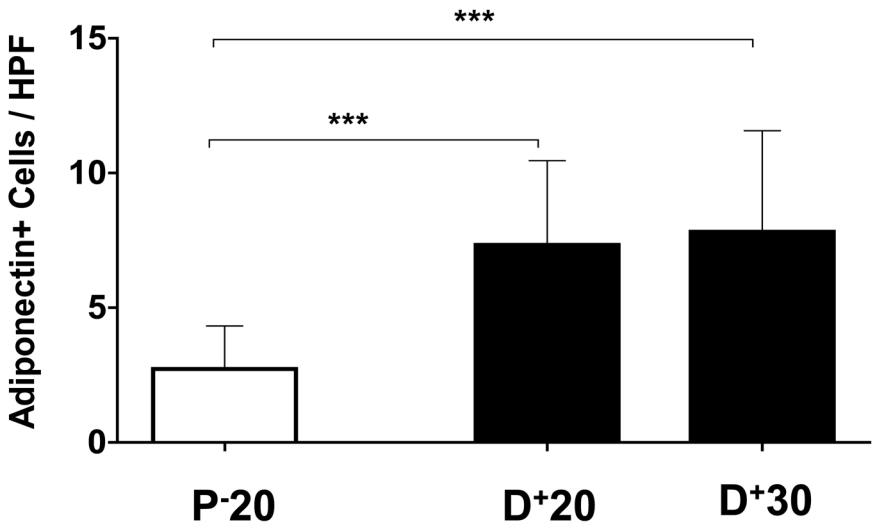

B

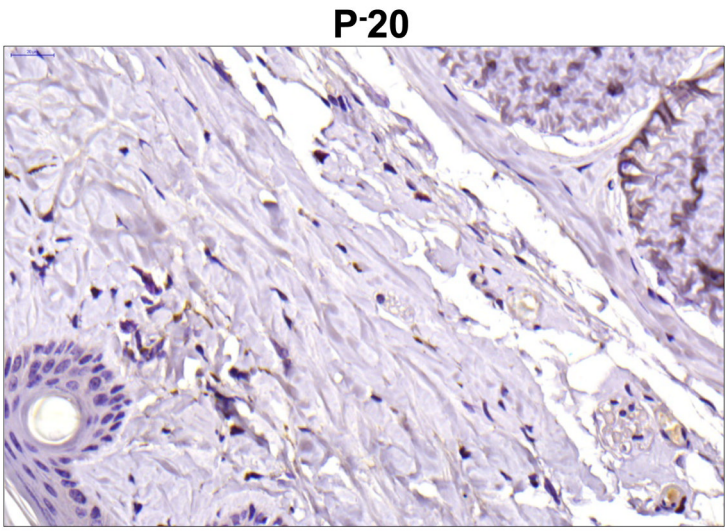

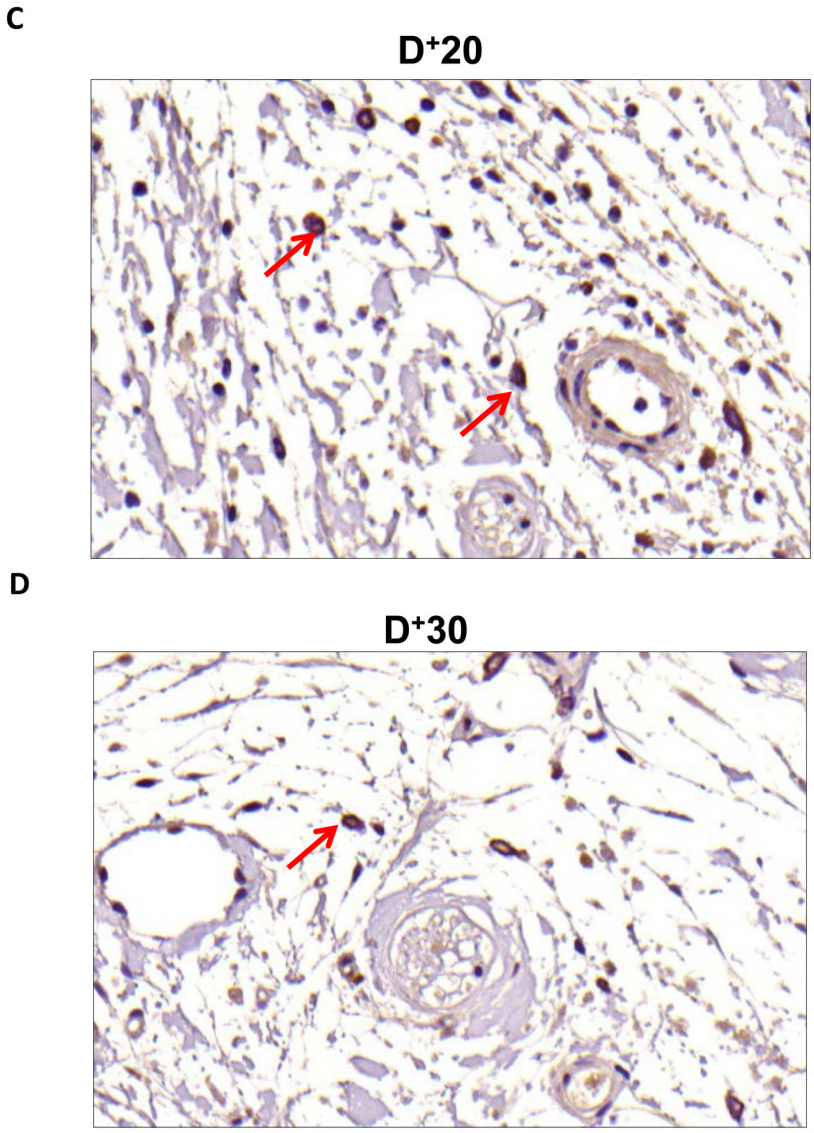

FIGURE 6. Gradients of lymphatic fluid stasis regulate the expression of adiponectin

A. Adiponectin^{+} cells/high powered field (HPF) cell counts in the various regions of the tail relative to the zone of lymphatic obstruction. Note significant increase in the number of adiponectin^{+} cells/HPF in distal sections (***$p<0.001$).

B–**D.** Representative high power (40x images of cross-sectional regions of the mouse tail relative to the zone of lymphatic obstruction stained for adiponectin. Note staining of mononuclear cells in subcutaneous fat in distal regions (red arrows).

A

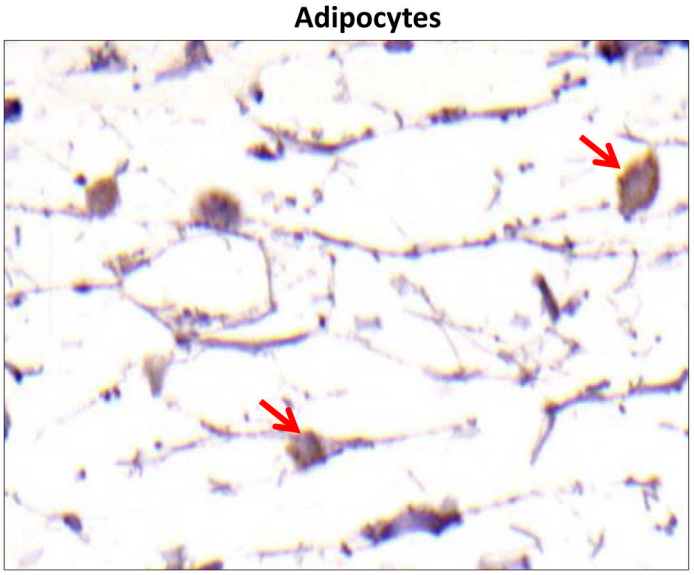

B

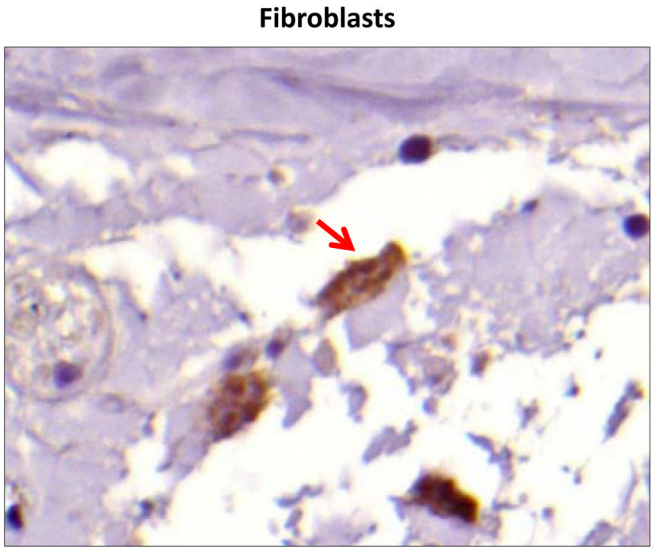

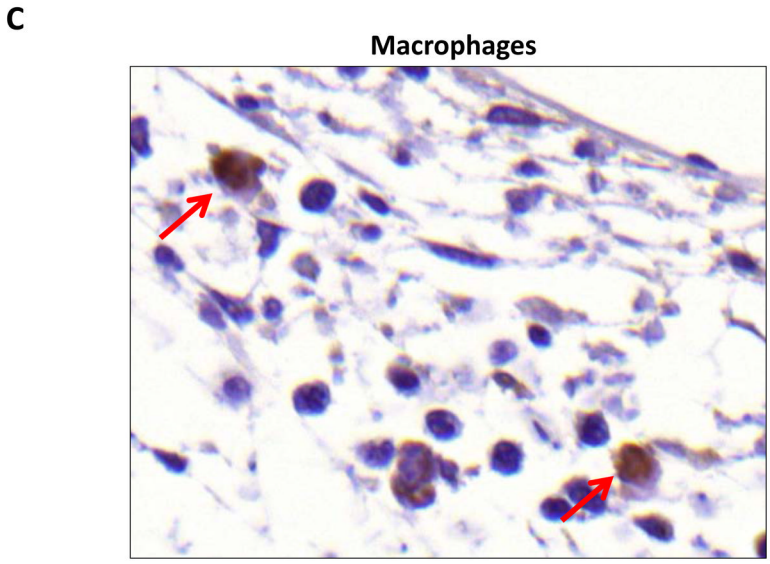

FIGURE 7. Adiponectin is expressed by a variety of cell types in response to lymphatic fluid stasis

A–C. Adiponectinstaining (red arrows) of adipocytes (A), fibroblasts (B), and macrophages shown in representative high power (80X) images of the distal region (D+20) of the tail.